



Publication Year	2002
Acceptance in OA @INAF	2023-01-03T11:39:38Z
Title	Observations of extragalactic masers in bright IRAS sources
Authors	TARCHI, ANDREA; Henkel, C.; Peck, A. B.; MOSCADELLI, Luca; Menten, K. M.
Handle	http://hdl.handle.net/20.500.12386/32825
Series	arxiv

Observations of extragalactic H₂O masers in bright IRAS sources

A. Tarchi¹, C. Henkel¹, A. B. Peck¹, L. Moscadelli² and K. M. Menten¹

¹ *Max-Planck-Institut für Radioastronomie, Auf dem Hügel 69, D-53121 Bonn, Germany*

² *Osservatorio Astronomico di Cagliari, Loc. Poggio dei Pini, Strada 54, 09012 Capoterra (CA), Italy*

Abstract. We report the first results of an ongoing survey at 22 GHz with the 100-m Effelsberg telescope to search for water maser emission in bright IRAS sources. We have detected water vapor emission in IC 342. The maser, associated with a star forming region $\sim 10\text{--}15''$ west of the nucleus, consists of a single 0.5 km s^{-1} wide feature and reaches an isotropic luminosity of $10^{-2} L_{\odot}$ ($D=1.8\text{ Mpc}$). Our detection raises the detection rate among northern galaxies with IRAS point source fluxes $S_{100\mu\text{m}} > 50\text{ Jy}$ to 16%.

1. Introduction

To date, luminous extragalactic H₂O masers can be grouped into three classes: those tracing accretion disks (e.g. NGC 4258); those in which the emission is either the result of an interaction between the radio jet and an encroaching molecular cloud or an accidental overlap, along the line-of-sight, between a warm dense molecular cloud and the radio continuum of the jet (e.g. NGC 1052 and Mrk 348); those related to prominent sites of star formation, such as the ones observed in M 33 (the earliest known extragalactic H₂O masers), and later also in IC 10.

Extragalactic H₂O masers are preferentially detected in nearby galaxies that are bright in the infrared ([4]). While nuclear masers are of obvious interest, non-nuclear masers are also important for a number of reasons: these sources allow us to pinpoint sites of massive star formation, to measure the velocity vectors of these regions through VLBI proper motion studies, and to determine true distances through complementary measurements of proper motion and radial velocity (e.g. [6]).

We have therefore observed the nearby spiral galaxies IC 342 and Maffei 2, both of which exhibit prominent nuclear bars and strong molecular, infrared,

and radio continuum emission. In the following we report the results of our observations.

2. Water maser observations of Maffei 2 and IC 342

2.1. The observation and image processing

The $6_{16} - 5_{23}$ line of H_2O (rest frequency: 22.23508 GHz) was observed with the 100-m telescope of the MPIfR at Effelsberg¹ toward Maffei 2 and IC 342. The full width to half power beamwidth was $40''$. The observations were carried out in a dual beam switching mode with a beam throw of $2'$ and a switching frequency of ~ 1 Hz. The pointing accuracy was always better than $10''$.

On May 12, 2001, IC 342 was observed with the Very Large Array² (VLA) in its B configuration. The 103 channels used, out of the 128 observed, cover a range in velocity of $\sim 8 \text{ km s}^{-1}$ centered at 16 km s^{-1} LSR (the velocity of the line detected at Effelsberg). No continuum subtraction was needed. The data were deconvolved using the CLEAN algorithm ([10]). The restoring beam is $0''.4 \times 0''.3$ and the rms noise per channel is $\sim 10 \text{ mJy}$, consistent with the expected thermal noise.

2.2. Results

Our single-dish observations towards Maffei 2 yielded no detection, with a 5σ upper limit of 25 mJy (channel spacing: 1.05 km s^{-1} ; velocity range: $-250 \text{ km s}^{-1} < V < +230 \text{ km s}^{-1}$; epoch: Apr 3, 2001; position: $\alpha_{2000} = 02^{\text{h}} 41^{\text{m}} 55^{\text{s}}.2$, $\delta_{2000} = +59^\circ 36' 11''$).

On April 2, 2001, we obtained the first definite detection of water vapor emission in IC 342. During the next night the detection was confirmed with a velocity resolution sufficient to resolve the line profile (Fig. 1a). The detected feature lies at $V_{\text{LSR}} = 16 \text{ km s}^{-1}$ and has a linewidth of $\sim 0.5 \text{ km s}^{-1}$; on April 2, no other component was seen at velocities $-175 \text{ km s}^{-1} < V < +310 \text{ km s}^{-1}$ (channel spacing: 1.05 km s^{-1} ; 5σ noise level: 16 mJy). A high line intensity ($\sim 100 \text{ mJy}$) and good weather conditions allowed us to map the emitting region (Fig. 2). Further measurements were performed on April 22 and May 7 (Fig. 1b & 1c). It is noticeable a fading in the peak and integrated intensities and a blue-shift in the velocity of the line by $\sim 1 \text{ km s}^{-1}$. Unfortunately, no emission above $\sim 30 \text{ mJy}$ (3σ level; 0.08 km s^{-1} channel spacing) was detected in the 22 GHz VLA B-array data taken on May 12. This fading by at least a factor of 3 within 5 days implies a size scale of $\lesssim 1.5 \times 10^{16} \text{ cm}$ ($\lesssim 900 \text{ AU}$) or $\lesssim 0.5 \text{ mas}$

¹The 100-m telescope at Effelsberg is operated by the Max-Planck-Institut für Radioastronomie (MPIfR) on behalf of the Max-Planck-Gesellschaft (MPG).

²The National Radio Astronomy Observatory is a facility of the National Science Foundation operated under cooperative agreement by Associated Universities, Inc.

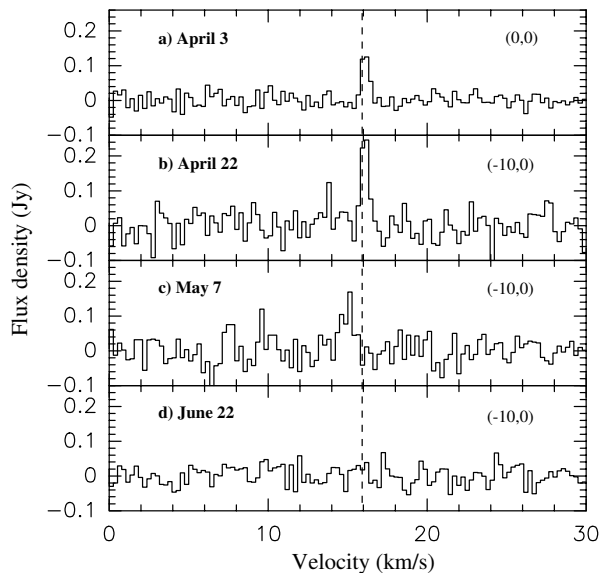


Figure 1. The H_2O maser feature observed with high velocity resolution (channel spacings after smoothing four contiguous channels are 0.26 km s^{-1}) on **a)** April 3, **b)** April 22, **c)** May 7, and **d)** June 22. The first spectrum has been taken at the $(0'', 0'')$ position, the others at $(-10'', 0'')$ relative to the position given in footnote ‘a’ of Table 1. The dashed line indicates $V_{\text{LSR}} = 16 \text{ km s}^{-1}$.

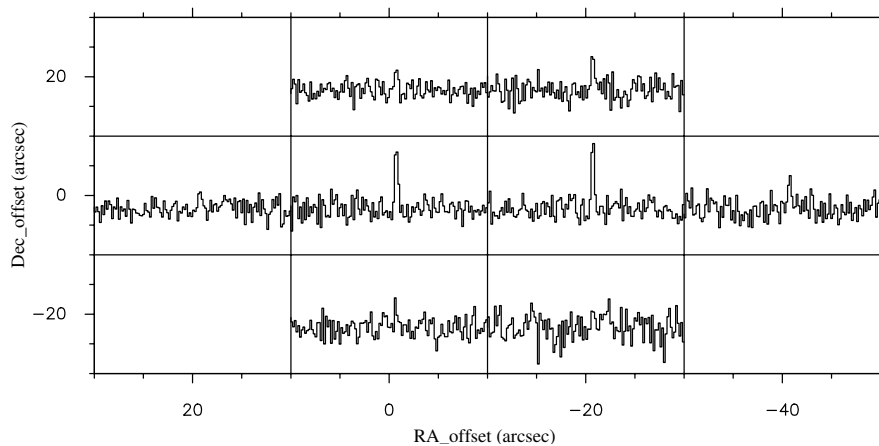


Figure 2. H_2O spectra obtained toward the central region of IC 342. Positions are offsets relative to $\alpha_{2000} = 03^{\text{h}}46^{\text{m}}48.6$ and $\delta_{2000} = +68^{\circ}05'46''$. Note that the spacing between two individual spectra ($20''$) is approximately half of the size of the 100-m Effelsberg telescope beam at 22 GHz ($40''$). Averaging four contiguous channels, the spectra have been smoothed to a spacing of 0.26 km s^{-1} .

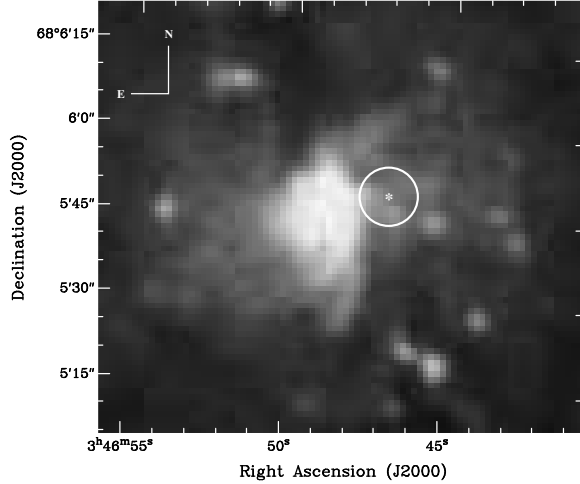


Figure 3. XDSS B-band image of the central region of IC 342. The asterisk indicates the water maser emitting position. The radius of the circle indicates its positional error as outlined in Sect. 3.2.

at a distance of 1.8 Mpc ([13]; see also Sect. 4.3); the corresponding brightness temperature is $\gtrsim 10^9$ K. The most recent spectrum was obtained on June 22 at Effelsberg (Fig. 1d). Confirming the VLA result, no maser signal was seen above 30 mJy (3σ ; channel spacing: 1.05 km s^{-1}).

Fitting a synthetic Gaussian to the data taken on April 3 (see Fig. 2), i.e. minimizing the sum of the difference squared between calculated and observed peak and integrated flux densities, we can obtain an accurate position of the emitting region: $\alpha_{2000} = 03^{\text{h}} 46^{\text{m}} 46^{\text{s}}.3$, $\delta_{2000} = +68^{\circ} 05'46''$. This is $13''$ to the west of our center position that coincides with the optical nucleus and the $2\mu\text{m}$ peak [14]; [1]. The accuracy of the derived maser position has been estimated to be $\sim 5''$.

2.3. Discussion

Arising from the central region of IC 342, but being displaced from the nucleus, the H_2O maser is likely associated with a prominent star forming region.

Fig. 3 shows an optical B-band image of the central region of IC 342, taken from the XDSS³. The maser emitting region (white circle) coincides with an

³The Digitized Sky Surveys were produced at the Space Telescope Institute under U.S. Government grant NAGW-2166. The images of these surveys are based on photographic data obtained using the Oschin Schmidt Telescope on Palomar Mountain and the UK Schmidt Tele-

arc-like structure extending E-S and is associated with a chain of sources that appear to be HII regions.

Occasionally, prominent galactic star forming regions show narrow ($\sim 0.5 \text{ km s}^{-1}$) flaring components that are exceptionally bright. Such flares were observed in W 31 A and W 49 ([12]; [11]). The prototype of these flares is the 8 km s^{-1} super maser in Orion-KL (e.g. [5]). During several months, the narrow highly linearly polarized maser reached flux densities in excess of 5 MJy. Surpassing the flux of any other velocity component by more than an order of magnitude and reaching a peak luminosity of $L_{\text{H}_2\text{O}} \sim 10^{-2} L_{\odot}$, the feature seems to be similar to that seen in IC 342. While luminosity, linewidth, and flux variations are reminiscent of the 8 km s^{-1} super maser in Orion-KL, our H_2O profiles show a significant velocity shift between April 22 and May 7 (Figs. 1b and c) that has not been seen in the Orion-KL flaring component. A simple model for explaining both the flare and the shift is, in our opinion, that the latter has a kinematic origin. Adopting a scenario of a chance alignment of two masing clouds along the line-of-sight, motion of the foreground relative to the background cloud along the plane of the sky and velocity structure in the foreground cloud could explain the observed data. A velocity gradient in the foreground cloud would then first shift the line velocity; once velocities are reached that are not matched within the background cloud, the flux density of the maser rapidly drops. Assuming that the distance between these clouds is $\ll 1.8 \text{ Mpc}$ and that their relative velocity in the plane of the sky is at the order of 100 km s^{-1} , this implies a cloud velocity gradient of up to $1 \text{ km s}^{-1}/\text{AU}$ during the time the source was monitored.

An almost identical scenario was proposed by [2] to account for the velocity shift of the flaring water maser component at -66 km s^{-1} in W49N. The similarity in velocity shift ($\sim 0.5 \text{ km s}^{-1}$) and time scale (58 days) of the event in W49N w.r.t the one in IC 342, indicates a common origin.

3. Extragalactic maser detection rates

While typical searches for extragalactic maser sources have only yielded detection rates between zero (e.g. [9]) and a few percent (e.g. [7]; [3]), there exists one sample with detection rates $>10\%$: These are the northern ($\delta > -30^\circ$) extragalactic IRAS (Infrared Astronomy Satellite) point sources with $100\mu\text{m}$ fluxes in excess of 50 Jy (for a source list, see [8]; Maffei 2 with $S_{100\mu\text{m}} \sim 200 \text{ Jy}$ should be added to the list). There is a total of 44 galaxies, two ultraluminous galaxies at intermediate distances (NGC 3690 and Arp 220) and 42 nearby sources ($V < 3000 \text{ km s}^{-1}$). Among these, seven (16%) are known to contain H_2O

scope. The plates were processed into the present compressed digital form with the permission of these institutions.

masers in their nuclear region. Two of these contain megamasers (NGC 1068 and NGC 3079), two are possibly nuclear kilomasers (NGC 253 and M 51; for details, see Sect. 1), and three are associated with prominent sites of star formation (IC 10, IC 342, M 82). Among the subsample of 19 sources with $100\mu\text{m}$ fluxes in excess of 100 Jy, five were so far detected in H_2O , yielding a detection rate in excess of 20%. Since few deep integrations have been obtained toward these sources, more H_2O detections can be expected from this promising sample in the near future.

Acknowledgments. We wish to thank Nikolaus Neininger for useful discussion. We are also indebted to the operators at the 100-m telescope, and to Michael Rupen and the NRAO analysts, for their cheerful assistance with the observations.

References

- [1] Becklin, E.E., Gatley, I., Matthews, K., Neugebauer, G., Sellgren, K., et al. 1980, *ApJ* *236*, 441
- [2] Boboltz, D.A., Simonetti, J.H., Dennison, B., Diamond, P.J., & Uphoff, J.A. 1998, *ApJ* *509*, 256
- [3] Braatz, J.A., Wilson, A.S., & Henkel, C. 1996, *ApJS* *106*, 51
- [4] Braatz, J.A., Wilson, A.S., & Henkel, C. 1997, *ApJS* *110*, 321
- [5] Garay, G., Moran, J.M., & Haschick, A.D. 1989, *ApJ* *338*, 244
- [6] Greenhill, L.J., Moran, J.M., Reid, M.J., Menten, K.M., & Hirabayashi, H. 1993, *ApJ* *406*, 482
- [7] Henkel, C., Güsten, R., Downes, D., Thum, C., Wilson, T.L., et al. 1984, *A&A* *141*, L1
- [8] Henkel, C., Wouterloot, J.G.A., & Bally, J. 1986, *A&A* *155*, 193
- [9] Henkel, C., Wang, Y.P., Falcke, H., Wilson, A.S., & Braatz, J.A. 1998, *A&A* *335*, 463
- [10] Högbom, J.A. 1974, *A&AS* *15*, 417
- [11] Lekht, E.E., Mendoza-Torres, E., & Sorochenko, R.L. 1995, *ApJ* *443*, 222
- [12] Liljeström, T., Mattila, K., Toriseva, M., & Anttila, R. 1989, *A&AS* *79*, 19
- [13] McCall, M.L. 1989, *AJ* *97*, 1341
- [14] van der Kruit, P.C. 1973, *A&A* *29*, 249